

VARIABILITY OF FREEZING LEVELS, MELTING SEASON INDICATORS, AND SNOW COVER FOR SELECTED HIGH-ELEVATION AND CONTINENTAL REGIONS IN THE LAST 50 YEARS

HENRY F. DIAZ¹, JON K. EISCHEID², CHRIS DUNCAN³ and
RAYMOND S. BRADLEY³

¹*Climate Diagnostics Center, NOAA, 325 Broadway, Boulder, CO 80305, U.S.A.
E-mail: hfd@cdc.noaa.gov*

²*Cooperative Institute for Research in Environmental Sciences, University of Colorado,
Boulder, CO 80309, U.S.A.*

³*Department of Geosciences, University of Massachusetts, Amherst, MA 01003, U.S.A.*

Abstract. We have used NCEP/NCAR Reanalysis data and a Northern Hemisphere snow cover data set to analyze changes in freezing level heights and snow cover for the past three to five decades. All the major continental mountain chains exhibit upward shifts in the height of the freezing level surface. The pattern of these changes is generally consistent with changes in snow cover, both over the course of the year and spatially. We examined different free-air temperature parameters (dry bulb temperature, virtual temperature, and 700–500 hPa thickness) using the Reanalysis grid point values located over the different mountain areas as defined in this study. The different trend values were in reasonably good agreement with each other, particularly over the second half of the record. Freezing level changes in the American Cordillera are strongly modulated by the El Niño/Southern Oscillation (ENSO) phenomenon and the freezing level heights (FLH) respond to both interannual and decadal-scale change in tropical Pacific sea surface temperature (SST). The ~ 0.5 °C increase in SST recorded in the tropical Pacific since the 1950s accounts for approximately half of the increase in FLH in tropical and subtropical latitudes of the Cordilleran region during that same time.

1. Introduction

In the last 20 years, a great deal of interest has been focused on climatic variations and changes in the mountain regions of the Earth, and on the effects of such changes on water resources, economic development, and ecosystem health, to name just a few impact areas (Beniston, 1994; Beniston et al., 1997; Messerli and Ives, 1997; Mountain Agenda, 1998). The Intergovernmental Panel on Climate Change (IPCC) considered the potential impacts of climate change on mountain regions as part of its Second Assessment Report (Beniston and Fox, 1995). In the IPCC Third Assessment Report (IPCC, 2001) there are several chapters, which touch upon the effects of global climate change in mountainous regions (e.g., in Chapters 4 and 5, on hydrology and water resources, and ecosystems, respectively).

Studies by Diaz and Graham (1996), Diaz and Bradley (1997), Parmesan et al. (1999), Thompson (2000), Pounds et al. (1999), and Still et al. (1999), for



Climatic Change **59**: 33–52, 2003.

© 2003 Kluwer Academic Publishers. Printed in the Netherlands.

example, demonstrate that the alpine zone can be quite sensitive to large scale climatic change, such that regional indices often show larger amplitudes relative to hemispheric or global averages. These and other studies (e.g., Dettinger and Cayan, 1995; Swetnam and Betancourt, 1998; Dyrgerov and Meier, 2000; Cayan et al., 2001; Dey, 2002) indicate the potential for significant changes in the timing of snowmelt in the alpine regions, including the disappearance of glaciers from high tropical regions of Africa and South America, and the risk of major ecological changes to some tropical cloud forest ecosystems and to temperate and subtropical latitude upland regions in both hemispheres.

In this study, we examine a number of indicators of climatic variations in selected high elevation regions. These include changes in the elevation of the free-air freezing level surface, in melting degree-days, and in snow cover. The data and methods are discussed in the next section, followed by a discussion of our results, and by a section summarizing our major findings.

2. Data and Methods

The height of the freezing level surface (FLS) – the elevation above sea level at which the air temperature is close to 0°C – is an important parameter, because it denotes the approximate position of permanent ice and snow on the surface, and thus constitutes an important indicator of climate variability and change. This analysis of freezing level changes for major mountain regions of the globe is based on a 53-year record (1948–2000) of free atmospheric temperatures from the NCEP/NCAR Reanalysis data set (Kistler et al., 2001). Biases introduced into the Reanalysis data set due to changes in observing platforms and data coverage have been discussed elsewhere (e.g., Santer et al., 1999; Trenberth et al., 2001; and Kistler et al., 2001). In general, we restrict our analyses to the period 1958 to present. We note that independent comparisons of different Reanalysis variables with other data sets, and with atmospheric GCM simulations forced with observed SST suggest that this period is reliable for most types of analysis. Our choice of analysis record is also supported by our own comparison of Reanalysis-derived indices with different parameters as described below.

As one major focus of this study is concerned with changes in freezing level heights and its potential impacts on glacier mass balances, we examined other important related indicators of the liquid/solid phase of water, such as annual totals of melting degree-days (MDD) – the cumulative sum of the difference between daily mean temperature and 0°C – for different high elevation regions. Note that this index is similar in construction to heating and cooling degree-days. MDDs accumulate only when the mean daily temperature exceeds 0°C . A set of daily MDDs was computed at the model-specified land surface level of the Reanalysis gridpoint and accumulated into monthly values. Since the horizontal Reanalysis model grid resolution is ~ 210 km, and we wished to calculate the MDD index in re-

gions of specially mountainous topography, a second version of the MDD data was computed at the model level corresponding to the median elevation of the surface topography (in general higher than the nominal model surface elevation), whose value within the Reanalysis grid was determined from the ETOPO5 (5-minute resolution) digital elevation model (DEM). The ETOPO-5 digital data base of land and sea-floor elevations on a 5-minute latitude/longitude grid (NGDC, 1988) is available through the National Geophysical Data Center, NOAA, in Boulder, Colorado (accessible via website: <http://www.ngdc.noaa.gov/mgg/global/etopo5.HTML>).

Changes in land surface area lying above the FLS at each grid of the Reanalysis data set were computed using ETOPO5 ground elevations to define high elevation regions. For each Reanalysis grid cell with mean monthly temperature lower than 0 °C, we summed the areas of all corresponding 5-minute land cells. We analyzed the regions of the world with highest topography (excluding Antarctica and Greenland, since our interest here is focused on the major mountain regions of the globe, where widespread glacier retreat has been documented in the past – see review by Thompson (2000)). We also paid particular attention to changes over the American Cordillera, because of the strong impact that the El Niño/Southern Oscillation (ENSO) phenomenon has in the western hemisphere, and because of previous work on Andean glaciers (Thompson, 2000; Thompson et al., 2000a,b), and on freezing level height changes related to SST changes in the tropical Pacific (Diaz and Graham, 1996; Vuille and Bradley, 2000; Vuille et al., 2003, this volume).

Snow cover is a closely related but independent indicator of climate and climate change. Northern Hemisphere snow cover has been mapped on a weekly basis by NOAA since late 1966. The NOAA charts indicate the presence or absence of snow each week by assigning a 1 or a zero to each cell in an 89×89 grid constructed on a polar stereographic projection (cell size varies from about 40,000 square kilometers at the pole to about 10,000 square kilometers at the grid corners near the equator). We use a version of the weekly snow cover charts for the period 1967–1999, processed and validated by the Rutgers University Climate Lab, following procedures outlined in Robinson (1991, 1993). For use in this study, we have averaged the data in time (by month) and space (onto the same 2.5×2.5 degree grid used for the NCEP/NCAR Reanalysis data), giving the mean snow covered area for each month for each Reanalysis cell.

3. Results

3.1. CHANGES ALONG THE AMERICAN CORDILLERA

The location of the NCEP/NCAR Reanalysis grids that are defined as comprising the American Cordillera region is illustrated in Figure 1; these boxes approximate the location of the mountainous topography in the Americas. Also shown are the median and 95% ground surface elevation profiles (the latter, shown to illustrate

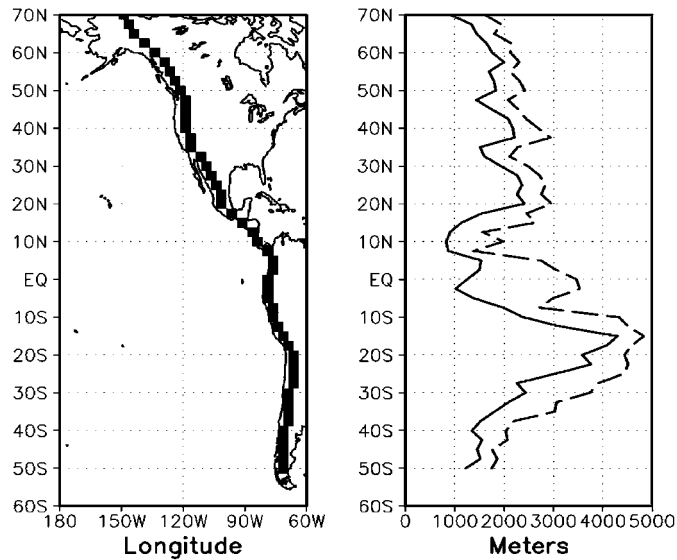


Figure 1. Location of NCEP/NCAR Reanalysis grid rectangles along the axis of high terrain of the North and South American Cordillera (left panel), and ground elevation profiles for the median (solid line) and 95th percentile 5-min resolution ground elevation values along this transect.

the elevation of the higher terrain in this region) for these grid quadrangles based on the ETOPO-5 data.

Initially, we performed a principal components analysis of the time series of freezing level height (FLH) associated with the transect of gridboxes shown in Figure 1. The results, illustrated in Figure 2, indicate that the freezing level surface varies coherently in the tropics, and that its temporal variability is largely controlled by the ENSO phenomenon – the zero-lag correlation between the American Cordillera FLH PC 1 time series in Figure 2 (lower panel), and monthly equatorial Niño-3 (Rasmusson and Carpenter, 1982) sea surface temperature (SST) is 0.67 ($N = 636$ months), significant at better than the 1% level. Maximum correlation, however, is reached with SST leading FLH by 2–3 months ($r = 0.75$).

In Figure 3, we provide further evidence of the strong association between tropical FLH (and hence mid-tropospheric temperature) in the American Cordillera and ENSO. Here, we have plotted the time evolution of monthly FLH and MDD along the American Cordillera from 20° N–20° S, against monthly Niño-3 SST. The FLH and SST series (top panel) are shown for 1948–2000; the MDD series goes through 1998 (see below). As noted above, maximum correlations between the two atmospheric series and Niño-3 SST occur with the latter leading the former by 2–3 months* ($r = 0.75$; $N = 636$ months), which are highly statistically

* The zero lag correlation coefficient between SST and FLH is 0.66; it is 0.39 with FLH leading SST by 3 months. The corresponding values for SST vs. MDD are 0.70 at zero lag and 0.44 for MDD leading SST by 3 months.

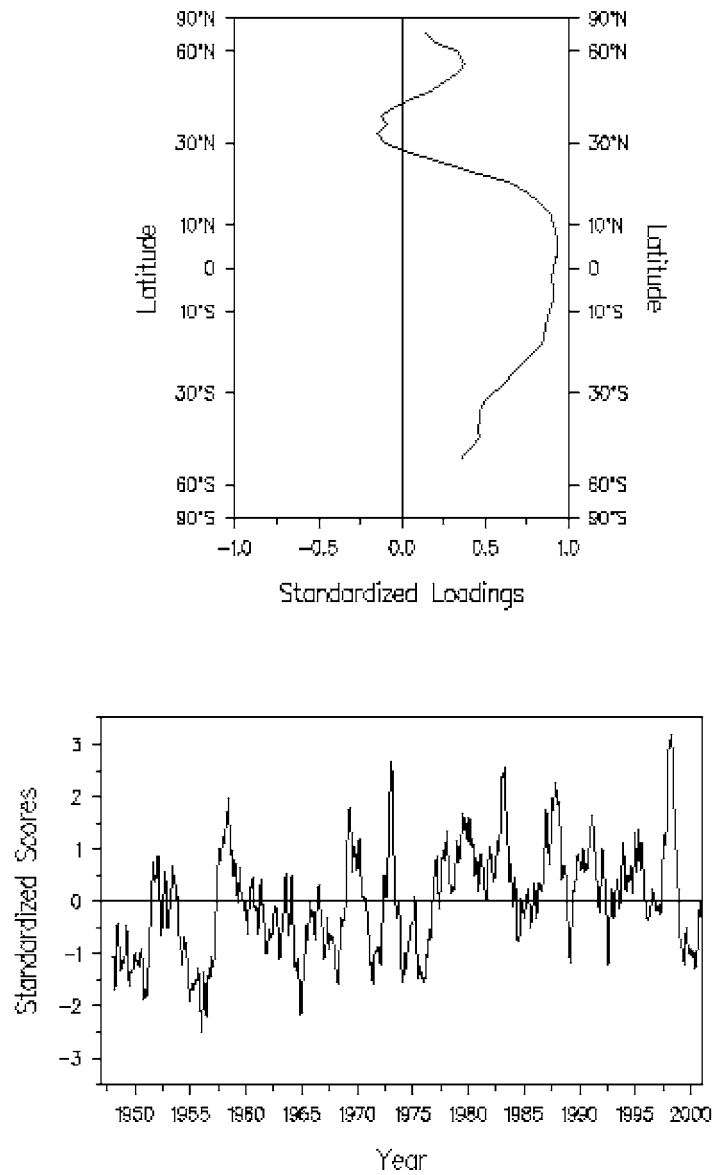


Figure 2. First principal component loadings (top graph) of monthly FLH along the western American Cordillera (Figure 1), and associated PC scores at the bottom. The first principal component accounts for 35% of the total freezing level height variability along the mountain transect.

significant. The pre-1958 data may contain biases, particularly in the Southern Hemisphere, arising from changes in the observing system (Kistler et al., 2001). However, we note that the cooler temperatures and lower FLH evident for these early years of the record are consistent with the generally lower (by about 0.5°C) tropical Pacific SST during that time (Diaz et al., 2001). The climate record produced by Thompson and his colleagues (see Thompson, 2000, and Thompson et al., 2003, this volume) from ice cores of major tropical glaciers in the high Andes of South America are located largely between 10°S and 30°S . For comparison, the lower panel of Figure 3 shows the FLH series corresponding to this highest segment of the American Cordillera from 10°S – 30°S (elevation profile, Figure 1). The correlation coefficient between FLH in this high topography segment and the tropical FLH series, shown in the top panel is 0.63 (0.65 for the period 1958–2000), significant at better than the 1% level.

For the period 1948–2000, tropical (20°N – 20°S) FLH increased by about 73 m (1.43 m/year) and from 1958–2000 FLH increased by 53 m (1.17 m/year). Linear regression of the FLH data on the Niño-3 SST values shows a change of about 76 m in FLH per $^{\circ}\text{C}$ change in SST. The Niño-3 SSTs have warmed by $\sim 0.5^{\circ}\text{C}$ since about 1950, so the increase in tropical Pacific SST directly accounts for at least 50% of the changes in Cordilleran FLH (Vuille et al., 2000a,b). Diaz and Graham (1996) documented trends in FLH in the tropics for the period 1970–86 of about 72 m, or about 4.5 m/yr (Figure 3). The slower rates of change over longer periods of time are consistent with the reduced rates of change reported by Gaffen et al. (2000); see also Seidel and Free, this issue. In particular, Seidel and Free point out that while there have been smaller changes in tropical freezing level heights since about 1980 (apart from interannual, ENSO-scale variations); tropical radiosonde data for the last 30 years or so, do show enhanced warming at higher elevation sites compared to nearby low elevation locations. We also note that the recent 3-year (La Niña) episode of lower ocean temperatures in the Pacific has depressed FLH in most of the tropics (and particularly in the Americas).

In terms of melting degree-days, both MDD and FLH curves display essentially the same type of temporal behavior and a high correlation with equatorial Pacific SST. However, the net change in mean monthly MDD from 1948–2000 for the tropical region (middle panel of Figure 3) is rather small, amounting to only about +2% of that mean, and the value for the period 1958–2000 is negligible.

We repeated the analysis of MDD changes for a subset of gridpoints located along the highest terrain in the South American Andes from 10°S to 30°S (Figure 1), generally corresponding to the region analyzed by Vuille and Bradley (2000). This high elevation subset (with a mean elevation of 3430 m) has a mean annual temperature of -0.1°C . The MDD trend for this high elevation subregion (not shown) is similar to that for the full tropical region, and displays similar temporal characteristics compared to FLH (bottom panel of Figure 3).

In the above discussion and in the following sections, we have left out an analysis of the freezing height behavior for the Canadian and U.S. cordilleran sectors.

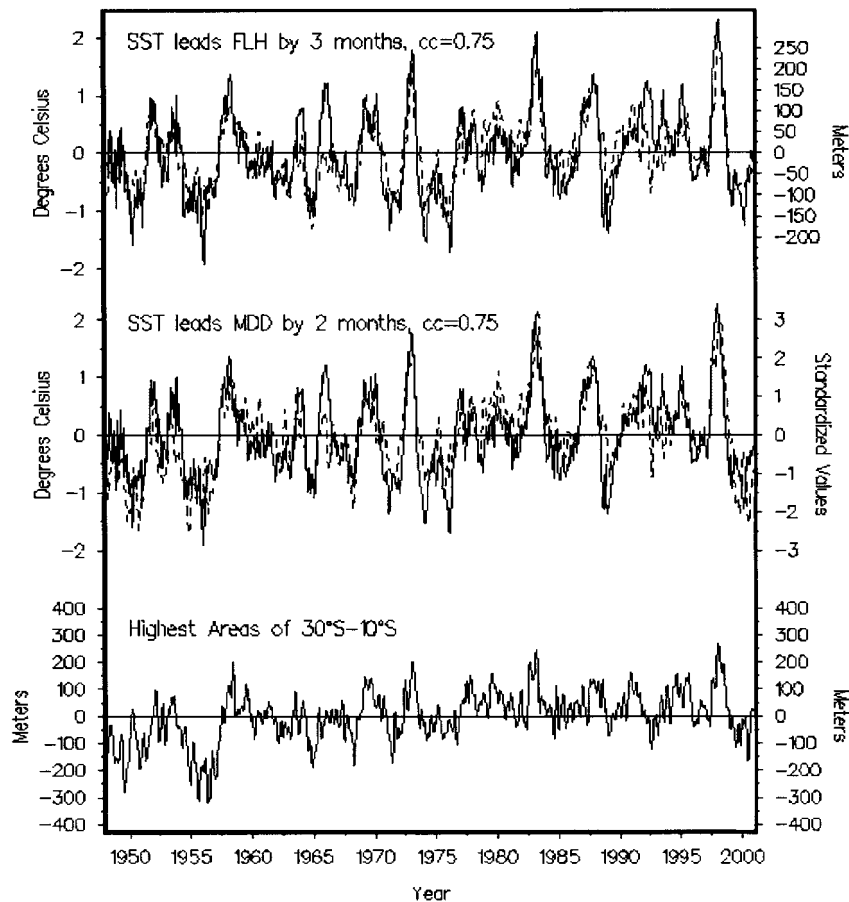


Figure 3. Time series of monthly FLH (top panel) anomalies and (middle panel) melting degree-day (MDD) anomalies at the land surface level within each Reanalysis cell along the American Cordillera from 20° N to 20° S (see Figure 1), plotted against Niño-3 SST anomalies (solid curve). The SST scale (°C) is on the left hand side; the scale for the FLH and MDD indices are on the right hand side, in meters for FLH and in standardized units for MDD (computed from the corresponding monthly means and standard deviations). The plotted FLH and MDD series (dashed lines) are shifted by 3-months and 2-months, respectively, with respect to the SST series. The bottom panel shows the FLH series along the highest points in the Cordillera, which are found from 10° S to 30° S.

We point the reader to the article by Diaz and Bradley (1997), which specifically analyzed surface temperature data for a set of high elevation stations (their Figures 2–4) in this region. For the U.S. Rockies, the authors found little trend in surface temperatures, but considerable decadal-scale variability. For the Canadian sector, a significant linear trend is present, amounting to about 1 °C since the late 1800s.

The magnitude of the temperature trends found by Vuille and Bradley (2000) – hereafter VB2000 – for the South American Andes, which showed the presence of continuing strong warming trends in the tropical Andes through 1998 (see also

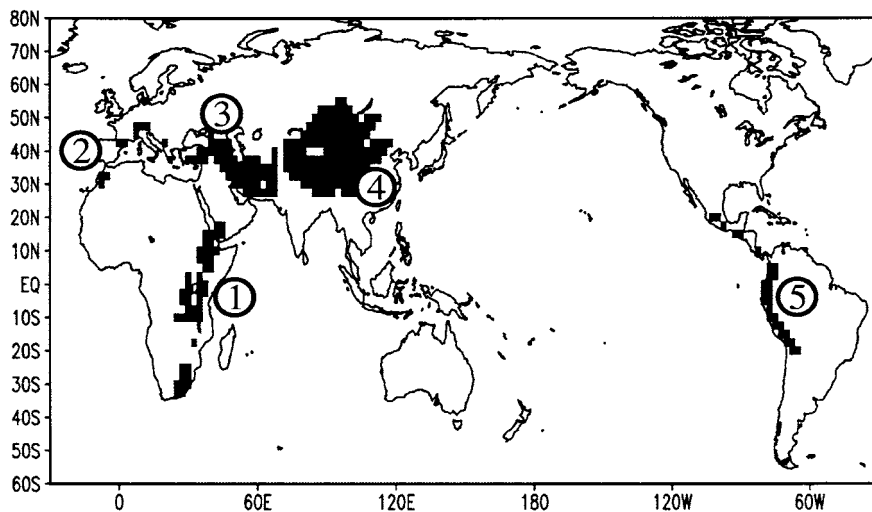


Figure 4. Map showing location of mountainous regions as discussed in the text. Region 1: East Africa, Region 2: Mediterranean (includes Atlas Mts., Alps), Region 3: Caucasus Mts., Region 4: Himalayas, Region 5: American Cordillera (includes only the tropical region).

Vuille et al., 2002, this issue), is comparable to those found in this study. Air temperature changes for the Cordillera region (Figure 4) for the period 1974–1998, used in VB2000, are comparable: 0.2°C in this study, versus 0.3°C in VB2000. In the following section we consider the surface temperature and freezing level changes in other mountainous areas of the globe.

3.2. CLIMATE TRENDS IN OTHER MOUNTAINOUS REGIONS

We defined five different regions over the globe with mountainous terrain (excluding Greenland and Antarctica): East Africa, a region stretching from the Atlas Mountains through the European Alps (labeled as Mediterranean), the region around the Caucasus, the Himalayas and the American Cordillera (Figure 4). These regions were defined in terms of Reanalysis gridpoints for which at least 95% of the 5-minute ground elevations (from the ETOPO-5 data) were above 1500 m. The surface temperature value was then derived from the model levels corresponding to the median value of the topography in that high elevation gridpoint, and averaged into the five regions illustrated in Figure 4. Linear trends (Figure 5) were calculated for the full 43-year period 1958–2000 and for a subset of years from 1974–1998, the latter period comprising a time of more rapidly rising temperatures and FLH change that comprises period studied by VB2000 using station data.

Table I gives the regional annual temperature correlations from Reanalysis data with land-only global, NH, and SH surface air temperature. The latter are based on a gridded version of the GHCN v.2 station data set (Peterson and Vose, 1997). Generally high correlations are found between the regional mountain temperature

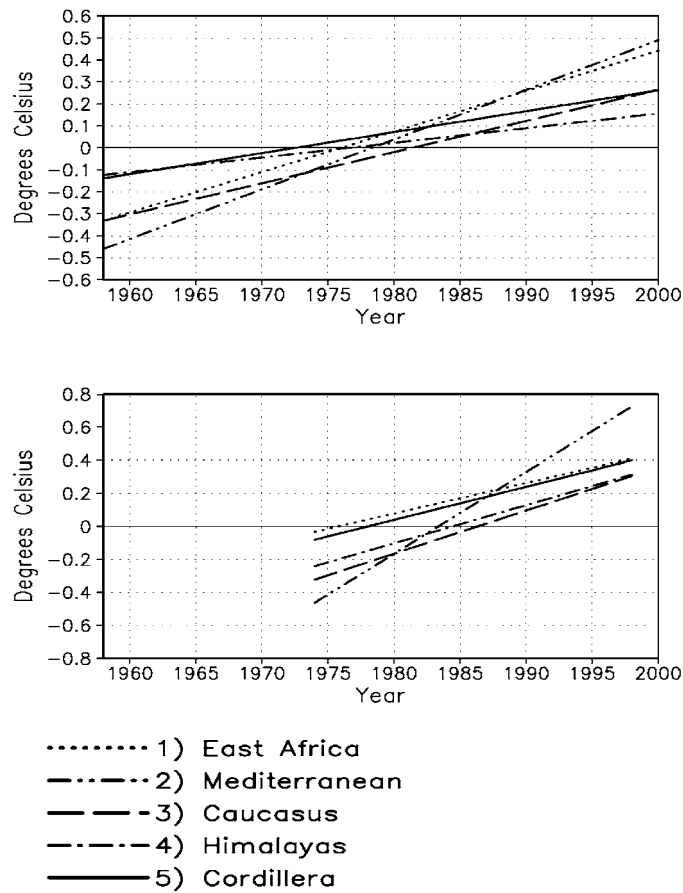


Figure 5. Linear trends in near surface air temperature for 5 different mountainous regions, based on the NCEP/NCAR Reanalysis data set. Top panel is for 1958–2000, lower panel for the period 1974–1998.

series (based on the Reanalysis data) and the hemispheric and global annual surface temperature variations (Quayle et al., 1999; Eischeid et al., 1995).

Table II summarizes the indicated period trends in these regions. Two other variables were calculated for these high elevation regions, to provide quasi-independent comparisons with the air temperature field. The virtual temperature (T_v) field, which provides a way to evaluate the effect of changes in humidity – an increase (decrease) in water vapor mixing ratios over the given intervals would cause a relative increase (decrease) in T_v . The 700–500 mb geopotential height thickness (situated ~ 3100 – 5600 m in height), gives another independent estimate of changes in mean layer temperature over a range of heights that is typical of these mountainous regions.

Over the longer 43-year record, increases in Reanalysis air temperature in these mountainous regions rise as little as $0.06^\circ\text{C}/\text{decade}$ (in the Himalayas), to as much

Table I

Pearson correlation matrix between annual air temperature series in five mountain regions and land-only global, NH and SH surface air temperature. Values are computed for the period 1948–2000 (first value), 1958–2000 (middle value), and 1974–1998 (third value)

	Global	NH	SH
E Africa	0.76/0.75/0.70	0.70/0.69/0.62	0.82/0.81/0.87
Mediterranean	0.72/0.73/0.77	0.71/0.72/0.74	0.61/0.60/0.76
Caucasus	0.53/0.62/0.69	0.53/0.60/0.65	0.44/0.52/0.74
Himalayas	0.70/0.73/0.80	0.68/0.69/0.77	0.64/0.70/0.81
Cordillera	0.64/0.60/0.73	0.55/0.51/0.68	0.86/0.85/0.85

Maximum number of observations: 53.

All correlation coefficients are statistically significant at the 1% level.

Table II

Linear trends in monthly mean values over the indicated periods. Air temps (first column) refers to the surface air temperature in the Reanalysis data. Second column gives the trend value for the virtual temperature parameter

Region	Air temps/virtual temps/700–500 mb thickness	
	1958–2000 ($N = 43$)	1974–1998 ($N = 25$)
East Africa	0.18 /0.09/ 0.54 (0.05)	<u>0.18</u> /0.21/ <u>0.70</u> (0.07)
Mediterranean	0.23 /–0.05/ 1.67 (0.17)	0.49 /0.08/ 3.49 (0.35)
Caucasus	0.14/0.03/ <u>0.63</u> (0.06)	0.26/0.19/1.05(0.11)
Himalayas	0.06/– 0.11 /– 0.79 (–0.08)	<u>0.23</u> /0.09/ 1.14 (0.11)
Cordillera	<u>0.09</u> /–0.02/ 0.97 (0.10)	<u>0.20</u> /–0.03/ <u>0.78</u> (0.08)
N. Hem. (surface)	0.15	0.28
S. Hem. (surface)	0.07	0.20

Air temperature trends are in °C/decade.

Thickness trends in m/decade. One m/decade thickness change translates into ~ 0.1 °C/decade temperature change in the 700–500 mb layer. The equivalent thickness-derived temperature change (in °C/decade) is shown next to the thickness trend in parentheses.

Statistically significant trends are shown in bold face at the 1% level, underlined at the 5% level.

as 0.23 °C/decade for the Mediterranean region. For the shorter period (1974–1998) the temperature trends range from 0.18 °C/decade over East Africa, to as much as 0.49 °C/decade in mountainous region of the Mediterranean. A study of mountain station pressure changes recorded for several mountain stations in different parts of the world was used to infer local and regional temperature changes by Toumi et al. (1999). The study, which made use of the hydrostatic equation and the measured

station pressures over many decades showed temperature changes in Europe and Asia that are compatible with our analysis.

Table II shows that corresponding virtual air temperature trends (which take into account changes in low-level humidity) differ substantially compared to corresponding changes in dry-bulb temperature over the period 1958–2000 (first two sets of values in the upper panel of Table II). The changes are more comparable for the 1974–1998 period, but the resulting differences point to the difficulty of modeling the surface boundary layer humidity. Virtual temperature trends are generally smaller than those for dry air temperature, suggesting the presence of drier conditions over time in these regions of high topographic relief. Trends in surface temperature for the five mountain regions examined here (Figure 4) are in much greater agreement with the temperature changes inferred from changes in the mean 700–500 mb layer thickness. The changes in 700–500 mb thickness over the 1958–2000 period translate to about 0.1 °C/decade, consistent with the results for air temperature.

For comparison, we also calculated the surface air temperature trends for the Northern and Southern Hemisphere land areas based on a gridded surface temperature data set (Peterson and Vose, 1997). The hemispheric scale changes are comparable to those obtained for the different major mountain regions (middle panel of Table II). Although it appears from this analysis that there's no consistent amplification of the warming signal in the major mountain zones, a greater rate of warming is evident in all the data sets for the 1974–1998 period.

3.3. TRENDS IN CONTINENTAL FLH

The pattern of evolution of the FLS might be considered a possible indicator of global climate change in the second half of the 20th century. We demonstrated above that along the spine of the American Cordillera, much of the temporal variability of FLH is associated with tropical Pacific SST variability. We expect that in association with the warming trends at high elevation, there should be an accompanying decrease in the surface areas situated above the freezing level.

The surface area inside each of the approximately 2.5-degree grid-boxes of the NCEP Reanalysis data that exceeded the height of the local FLS was tabulated for each year-month and period-of-record trends were computed. This is illustrated in Figure 6 for different regional aggregations for each calendar month, and the spatial patterns for the month with the highest negative areal trend in the Northern Hemisphere (April) is illustrated in Figure 7. We present the results in two ways: in terms of the estimated change in surface area above the freezing level (the top map in Figure 7), and as a percentage change with respect to the local mean value of the area above this level (bottom panel). Because of possible data and analyses biases in the first decade or so of the record (Kistler et al., 2001), here we present changes for the period of 1958–2000. While the overall annual change in surface area above the FLS in the period 1958–2000 is slightly negative (solid symbols on

the right vertical axis), there is evident seasonal heterogeneity in the trends. The largest decreases in the area above the FLS occurred in the Northern Hemisphere spring months (with a maximum area decrease in April).

Changes in Northern Hemisphere climate during its spring season have been documented by a number of investigators (e.g., Groisman et al., 1994; Dettinger and Cayan, 1995; Schwartz and Reiter, 2000; Cayan et al., 2001). Beginning in the northern autumn season, monthly changes tend to alternate between slightly positive and negative. Note that while, as expected, changes in total area above the freezing level are largest in the Northern Hemisphere (top panel in Figure 6), in terms of percentage change from mean values, the Southern Hemisphere (Figure 6, bottom panel) experiences the largest decline.

3.4. TRENDS IN SNOW COVERED AREA

Snow covered area (SCA) does not exactly match FLH patterns in space or in time due to the relative influences of varying moisture supply and the ability of snow cover to persist for some time after the FLS rises above the land surface. Differences in the patterns of SCA and FLH reflect these variations, but our analysis also shows similar patterns of change. In the following, we highlight regions where precipitation (as snowfall) and snowmelt changes have occurred over the past three decades (1967–1999), of available record.

The SCA trends for each calendar month for various regions (Figure 8) shows declining snow cover for all months except November and December, which show slight increases in SCA. The greatest total decline of SCA occurs in October, though all months from January through July have experienced declines of at least 50,000 km² per year over the 33-year record, most of that occurring in Eurasia. As a percentage of mean SCA, the greatest declines have occurred in June, July, August, and October. These changes compare favorably with those illustrated in the bottom panel of Figure 9 for Northern Hemisphere (NH) FLH trends over the same 1967–1999 period. NH FLH changes during that time also show a strong decline in area for the month of October, though the greatest changes occur in mid-winter and spring. However, as a percentage of the mean (Figure 9, lower panel), NH FLS area changes, like SCA, show the greatest declines in the summer.

The spatial patterns of SCA trends reveal seasonal differences in the SCA-FLH relationship as well. In April, where both SCA and FLS have been declining in the Northern Hemisphere, there is relatively strong spatial coherence of the regions of decline and increase (top two panels of Figure 10). The majority (70%) of the cells for which there is both snow cover and frozen ground show similar trends (both increasing, both decreasing, or both not changing very much). Of the remaining areas, North America and central Asia show areas with mostly steady to increasing SCA trends in areas of declining FLS area, which may be due to an increase in spring precipitation (as snowfall) even though a temperature increase is suggested by the FLH changes. Parts of south-central and eastern Asia show steady to de-

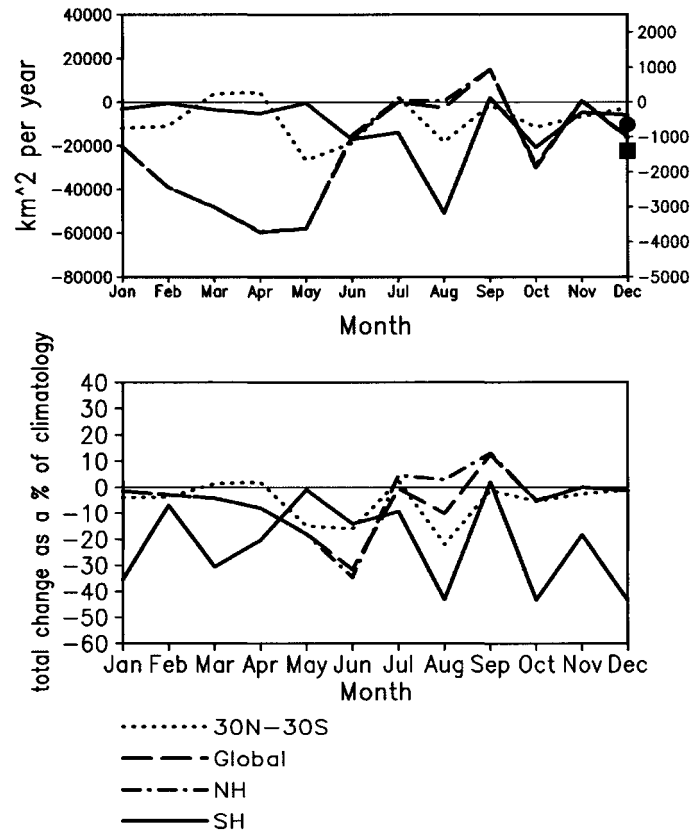


Figure 6. Change in surface area above the FLS over the period (1958–2000) by month for the Tropics (30° N–30° S), Northern (0–70° N), and Southern Hemisphere (0–50° S) (*Global curve, 50° S–70° N, excludes Greenland and Antarctica). Trends in the top panel are in units of square-kilometers per year, with mean annual changes denoted by a large solid square for the Northern Hemisphere, and a large solid dot for the Southern Hemisphere. Left-hand scale applies to global and NH trends, right-hand scale applies to Tropics and SH trends. The bottom panel gives the equivalent rate of change in percent of the climatological mean area above the freezing level for the grid areas in each region.

creasing SCA in areas of steady to increasing FLS coverage, which may mean a reduction in the rate of spring snowmelt or less snowfall in those places despite the presence of cooler temperatures.

The changes indicated in Figures 7–10, showing large declines in Northern Hemisphere snowcover and the lifting of the freezing level surface, coincide with a strong warming trend in the region of Eurasia and North America, where mean annual temperatures have increased by about 1 °C during the last century, mostly in the last 30 years (Figure 11). Figure 11 depicts a time series of annual surface temperatures departure from a 1951–1980 reference mean for the region where the climatological annual mean temperature is within ±1 °C of freezing (largely in

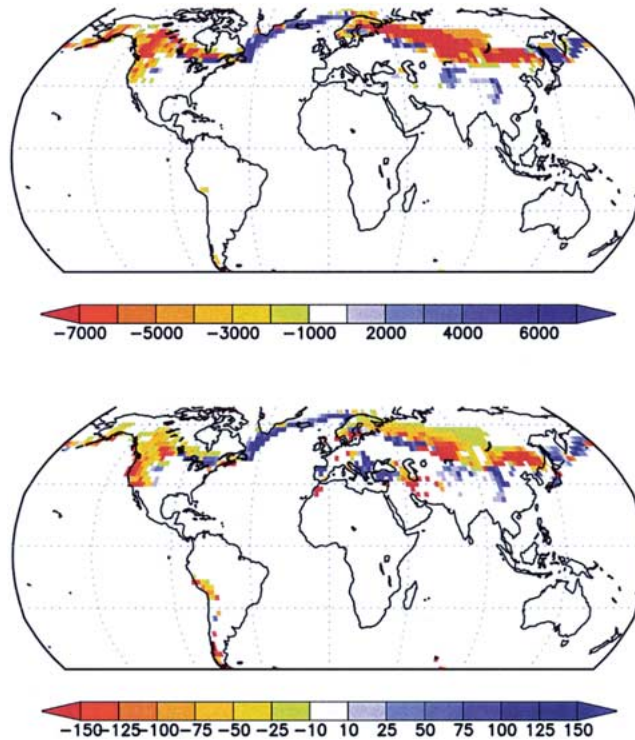


Figure 7. Map showing net changes in (top panel) surface area (km^2) above the FLS, and (bottom panel) expressed in percent of the long-term mean for each grid area. Data are for the month of April. Changes calculated for the period 1958 through 2000.

the Northern Hemisphere subarctic regions). The longer perspective provided by the surface temperature record in the subarctic indicates that most of the warming in the last 100 years occurred during the last 30 years, when the largest declines in areas intersecting the freezing level isotherm are noted (particularly from early spring to early summer) and substantial decreases in areas with spring snowcover are documented (particularly from early spring through summer).

4. Summary and Discussion

Increases in freezing-level height as a result of rising temperatures has led to a decline in the surface area of mountainous regions existing above this critical level. For the period 1958–2000, the greatest areal changes in FLH (which is analogous to equilibrium line altitudes) have occurred during the northern spring months (maximum changes in April, Figure 6). However, as a percentage of the mean coverage, land areas in the Southern Hemisphere north of 50° S also display changes comparable to those for the NH. FLH changes are widespread around the globe,

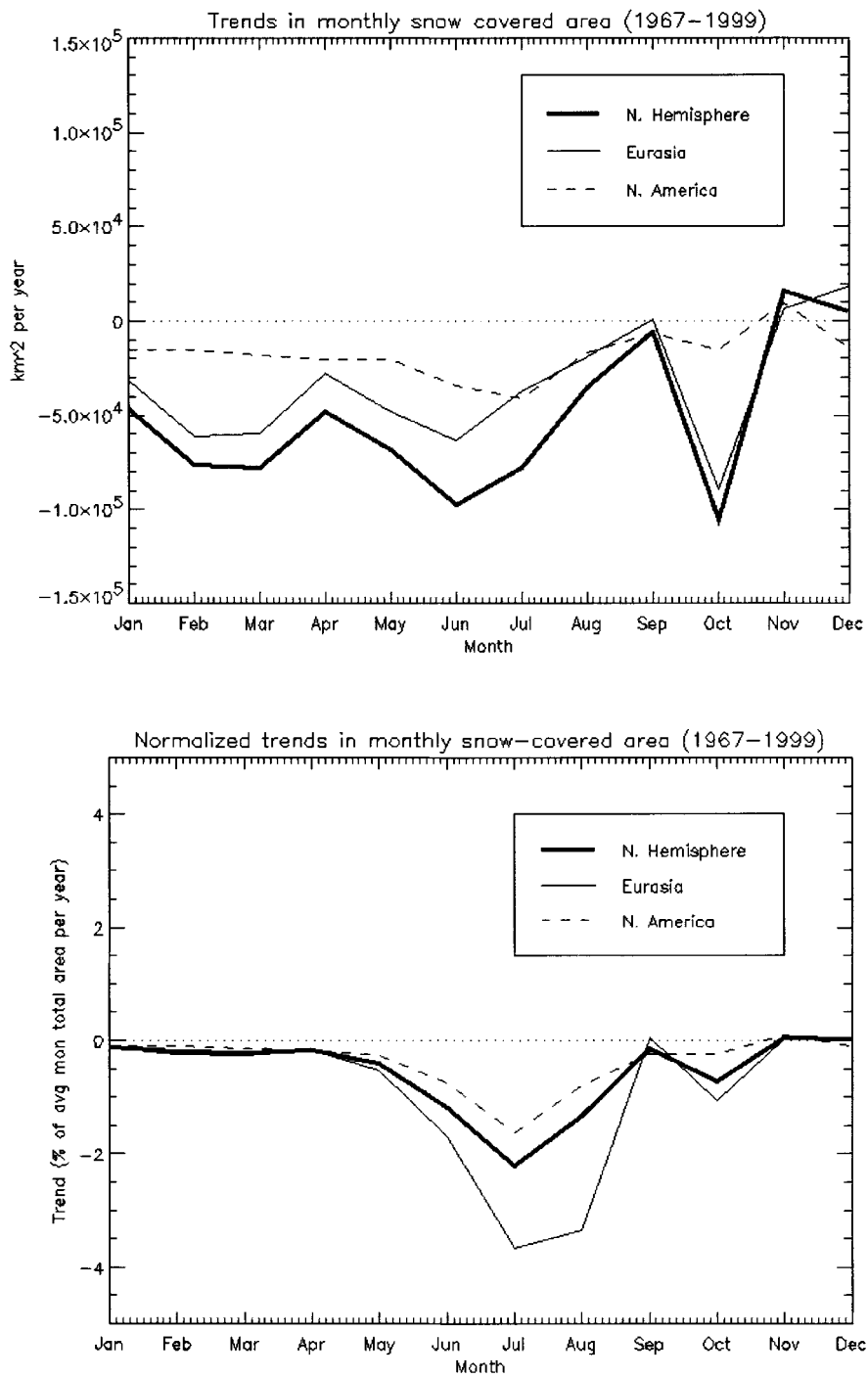


Figure 8. Same as Figure 6, but for snow covered area for the period 1967-1999.

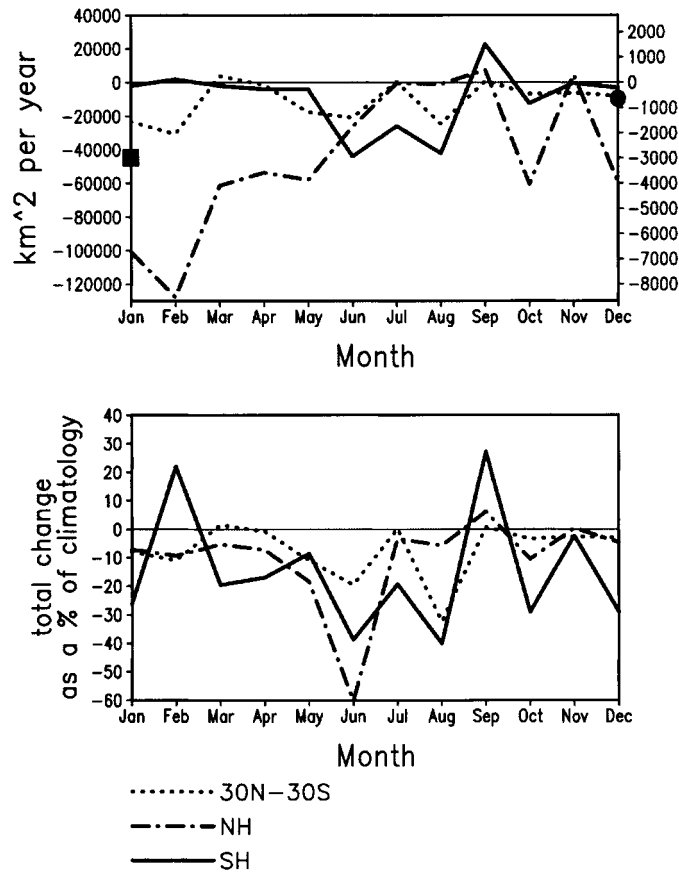


Figure 9. Same as Figure 6, but for the period 1967–1999 for direct comparison with Figure 8.

and the pattern of change resembles the change in surface air temperature that has been documented in other studies. The variations in temperature and FLH in the American tropics is strongly modulated by SST changes in the tropical Pacific associated with the ENSO phenomenon.

Similar trends are found in the total snow covered area (SCA) in the Northern Hemisphere for the period 1967–1999. Most months show significant declines in SCA, most notably October, similar to that for FLH in the Northern Hemisphere. Comparison of the spatial patterns of SCA and FLS changes suggest a coherent relationship between SCA and FLS in the spring, and, in those areas where the trends differ, reduced precipitation and/or snowmelt.

Multidecadal trends in near-surface temperature at five selected mountainous regions are similar in magnitude to global or hemispheric-scale values (+0.4 to 0.6 °C during second half of the 20th century). The question of the magnitude of climatic change in mountain regions relative to those nearer to sea level is an important issue that is still uncertain. We did not find from this analysis evidence

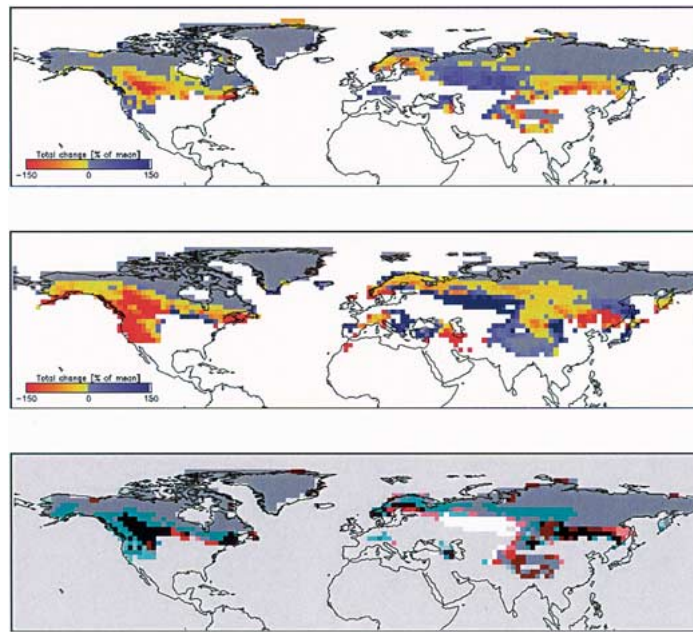


Figure 10. Maps showing net period-of-record (1967–1999) changes in (top panel) snow covered area (SCA) expressed as percentage of the long-term mean at each grid box, net changes in (middle panel) land surface area above freezing level (FLS), and relative changes in SCA and FLS (bottom panel; black = both declining; gray = both steady; white = both increasing; cyan shades = steady/increasing SCA, steady/declining FLS; red shades = steady/decreasing SCA, steady/increasing FLS; threshold for 'steady' = $\pm 20\%$ net change). Data is for the month of April.

for a consistent amplification of the surface large-scale warming signal in the major mountain zones. A greater rate of warming in the second half of the study period is evident in all the data sets. The rise in FLH in the last ~ 50 years may be related to higher SST in the Tropics, warming of the mid-troposphere, increases in humidity, and/or changes in precipitation.

Glacier recession for the past century has been documented by several investigators (e.g., Thompson, 2000; Thompson et al., 2000a–c; Meier et al., 2003). It has been suggested that the world's mountain regions represent one of the globe's critical large-scale systems that may be at increased risk from global climate change (Beniston, 2003; Diaz et al., 2003). Significant impacts resulting from climate changes are anticipated over the next few decades for mountain systems, such as alpine hydrology and ecology, and in the area of water resources management and the availability of adequate water supplies for human uses in regions of the world where most of the water-use comes from mountain snowmelt.

Mountain areas of the world have been called 'Water Towers for the 21st Century', and the recognition of the importance of mountain environments around the globe led to the designation of the year 2002 as the 'International Year of the Mountains' by the United Nations. International research programs have been ini-

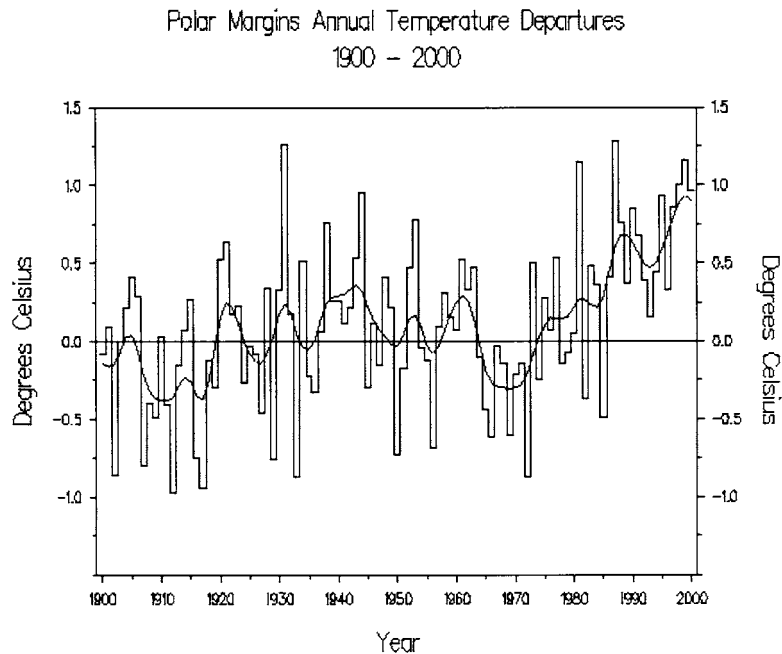


Figure 11. Time series of temperature departures from the long-term mean in regions where the mean annual temperature is within $\pm 1^\circ\text{C}$ of the freezing threshold (0°C).

tiated (Becker and Bugmann, 2001; Messerli and Ives, 1997) to promote integrated climate research and monitoring efforts in many of the world's mountain regions. These efforts underscore the need for integrated climate research efforts for the mountain regions in the United States.

Acknowledgements

We thank the reviewers for constructive criticisms and suggestions. H.F.D, J.K.E. and R.S.B were supported in part by Grant No. DE-AI03-01ER63134 of the Biological and Environmental Research Program (EBR), U.S. Department of Energy.

References

- Becker, A. and Bugmann, H. E. (eds.): 2001, *Global Change and Mountain Regions International Geosphere Biosphere Program Report No. 49*, Stockholm, p. 86.
- Beniston, M. (ed.): 1994, *Mountain Environments in Changing Climates*, Routledge, London and New York, p. 461.
- Beniston, M.: 2002, 'Climatic Change in Mountain Regions: A Review of Possible Impacts', *Clim. Change*, this issue.

- Beniston, M., Diaz, H. F., and Bradley, R. S.: 1997, 'Climate Change at High Elevation Sites: An Overview', *Clim. Change* **36**, 233–251.
- Beniston, M. and Fox, D. G.: 1995, 'Impacts of Climate Change on Mountain Regions', in Watson, R. T. Zinyowera, M. C., and Moss, R. H. (eds.), *Climate Change 1995, Impacts, Adaptations and Mitigation of Climate Change: Scientific-Technical Analyses*, published by Cambridge University Press (Cambridge) for the IPCC, pp. 191–213.
- Cayan, D. R., Kammerdiener, S. A., Dettinger, M. D., Caprio, J. M., and Peterson, D. H.: 'Changes in the Onset of Spring in the Wwestern United States', *Bull. Amer. Meteorol. Soc.* **82**, 399–415.
- Dye, D. G.: 2002, 'Variability and Trends in the Annual Snow-Cover Cycle in Northern Hemisphere Land Areas, 1972–2000', *Hydrol. Process.* **16**, 3065–3077.
- Dettinger, M. D. and Cayan, D. R.: 1995, 'Large-Scale Atmospheric Forcing of Recent Trends toward Early Snowmelt Runoff in California', *J. Climate* **8**, 606–623.
- Diaz, H. F. and Bradley, R. S.: 1997, 'Temperature Variations during the Last Century at High Elevation Sites', *Clim. Change* **36**, 253–279.
- Diaz, H. F. and Graham, N. E.: 1996, 'Recent Changes in Tropical Freezing Heights and the Role of Sea Surface Temperature', *Nature* **384**, 152–155.
- Diaz, H. F., Grosjean, M., and Graumlich, L. J.: 2003, 'Climate Variability and Change in High Elevation Regions: Past, Present and Future', *Clim. Change*, this issue.
- Diaz, H. F., Hoerling, M. P., and Eischeid, J. K.: 2001, 'ENSO Variability, Teleconnections, and Climate Change', *Int. J. Clim* **21**, 1845–1862.
- Dyrgerov, M. B. and Meier, M. F.: 2000, 'Twentieth Century Climate Change: Evidence from Small Glaciers', *Proc. Nat. Acad. Sci. U.S.A.* **97**, 1406–1411.
- Eischeid, J. K., Baker, C. B., Karl, T. R., and Diaz, H. F.: 1995, 'The Quality Control of Long-Term Climatological Data Using Objective Data Analysis', *J. Appl. Meteorol.* **34**, 2787–2795.
- Gaffen, D. J., Santer, B. D., Boyle, J. S., Christy, J. R., Graham, N. E., and Ross, R. J.: 2000, 'Multidecadal Changes in the Vertical Temperature Structure of the Tropical Troposphere', *Science* **287**, 1242–1245.
- Groisman, P. Y., Karl, T. R., Knight, R. W., and Stenchikov, G. L.: 1994, 'Changes in Snow Cover, Temperature, and Radiative Heat Balance over the Northern Hemisphere', *J. Climate* **7**, 1633–1656.
- Intergovernmental Panel on Climate Change: 2001, *Climate Change 2001, Impacts, Adaptation, and Vulnerability*, Cambridge University Press, Cambridge, p. 1032.
- Kistler, R., Kalnay, E., Collins, W., Saha, S., White, G., Woollen, J., Chelliah, M., Ebisuzaki, W., Kanamitsu, M., van den Dool, H., Jenne, R., and Fiorino, M.: 2001, 'The NCEP/NCAR 50-year Reanalysis: Monthly Means, CD-ROM and Documentation', *Bull. Amer. Meteorol. Soc.* **82**, 152–168.
- Meier, M., Dyrgerov, M., and McCabe, G.: 2003, 'The Health of Glaciers: Recent Changes in Glacier Regime', *Clim. Change*, this issue.
- Messerli, B. and Ives, J. D. (eds.): 1997, *Mountains of the World, a Global Priority*, The Parthenon Publishing Group, New York and London, p. 495.
- Moutain Agenda: 1998, *Mountains of the World, Water Towers for the 21st Century*, Institute of Geography, University of Berne, Switzerland, p. 32.
- National Geophysical Data Center, NOAA: 1988, 'Data Announcement 88-MGG-02, Digital Relief of the Surface of the Earth', Boulder, CO.
- Parmesan, C. and 12 others: 1999, 'Poleward Shifts in Geographical Ranges of Butterfly Species Associated with Regional Warming', *Nature* **382**, 579–583.
- Peterson, T. C. and Vose, R. S.: 1997, 'An Overview of the Global Historical Climatology Network Temperature Database', *Bull. Amer. Meteorol. Soc.* **78**, 2837–2849.
- Pounds, J. A., Fogden, M. P. L., and Campbell, J. H.: 1999, 'Biological Response to Climate Change on a Tropical Mountain', *Nature* **398**, 611–615.

- Quayle, R. G., Peterson, T. C., Basist, A. N., and Godfrey, C. C.: 1999, 'An Operational Near-Real-Time Global Temperature Index', *Geophys. Res. Lett.* **26**, 333–335.
- Rasmusson, E. M. and Carpenter, T. H.: 1982, 'Variations in Sea Surface Temperature and Surface Wind Fields Associated with the Southern Oscillation/El Niño', *Mon. Wea. Rev.* **110**, 354–384.
- Robinson, D.: 1991, 'Merging Operational Satellite and Historical Snow Cover Data to Monitor Climate Change', *Glob. Plan. Change* **90**, 235–240.
- Robinson, D.: 1993, 'Hemispheric Snow Cover from Satellites', *Ann. Glaciol.* **17**, 367–371.
- Santer, B. D., Hnilo, J. J., Wigley, T. M. L., Boyle, J. S., Doutriaux, C., Fiorino, M., Parker, D. E., and Taylor, K. E.: 1999, 'Uncertainties in Observationally Based Estimates of Temperature Change in the Free Atmosphere', *J. Geophys. Res.* **104**, 6305–6333.
- Schwartz, M. D. and Reiter, B. E.: 2000, 'Changes in North American Spring', *Int. J. Clim.* **20**, 929–932.
- Seidel, D. J. and Free, M.: 2003, 'Comparison of Lower-Tropospheric Temperatures at Low and High Elevation Radiosonde Sites', *Clim. Change*, this issue.
- Still, C. J., Foster, P. N., and Schneider, S. H.: 1999, 'Simulating the Effects of Climate Change on Tropical Montane Cloud Forests', *Nature* **398**, 608–610.
- Swetnam, T. W. and Betancourt, J. L.: 1998, 'Mesoscale Disturbance and Ecological Response to Decadal Climatic Variability in the American Southwest', *J. Climate* **11**, 3128–3147.
- Thompson, L. G.: 2000, 'Ice Core Evidence for Climate Change in the Tropics: Implications for our Future', *Quat. Sci. Rev.* **19**, 19–35.
- Thompson, L. G., Mosley-Thompson, E., and Henderson, K. A.: 2000a, 'Ice Core Paleoclimate Records in Tropical South America since the Last Glacial Maximum', *J. Quat. Sci.* **15**, 377–394.
- Thompson, L. G., Henderson, K. A., Mosley-Thompson, E., and Lin, P.-N.: 2000b, 'The Tropical Ice Core Record of ENSO', in Diaz, H. F. and Markgraf, V. (eds.), *El Niño and the Southern Oscillation, Multiscale Variability and Global and Regional Impacts*, Cambridge University Press, Cambridge, pp. 325–356.
- Thompson, L. G., Yao, T., Mosley-Thompson, E., Davis, M. E., Henderson, K. A., and Lin, P.-N.: 2000c, 'A High-Resolution Millennial Record of the South Asian Monsoon from Himalayan Ice Cores', *Science*, 1916–1919.
- Thompson, L. G., Mosley-Thompson, E., Davis, M. E., Lin, P.-N., Henderson, K. A., and Mashiota, T. A.: 2003, 'Tropical Glaciers and Ice Core Evidence of Climate Change on Annual to Millennial Time Scales', *Clim. Change*, this issue.
- Toumi, R., Hartell, N., and Bignell, K.: 1999, 'Mountain Station Pressure as an Indicator of Climate Change', *Geophys. Res. Lett.* **26**, 1751–1754.
- Trenberth, K. E., Stepaniak, D. P., and Hurrell, J. W.: 2001, 'Quality of Reanalysis in the Tropics', *J. Climate* **14**, 1499–1510.
- Vuille, M. and Bradley, R. S.: 2000, 'Mean Annual Temperature Trends and their Vertical Structure in the Tropical Andes', *Geophys. Res. Lett.* **27**, 3885–3888.
- Vuille, M., Bradley, R. S., and Keimig, F.: 2000a, 'Interannual Climate Variability in the Central Andes and its Relationship to Tropical Pacific and Atlantic Forcing', *J. Geophys. Res.* **105**, 12447–12460.
- Vuille, M., Bradley, R. S., and Keimig, F.: 2000b, 'Climatic Variability in the Andes of Ecuador and its Relationship to Tropical Pacific and Atlantic Sea Surface Temperature Anomalies', *J. Climate* **13**, 2520–2535.
- Vuille, M., Bradley, R. S., and Keimig, F.: 2003, '20th Century Climate Change in the Tropical Andes', *Clim. Change*, this issue.

(Received 21 March 2002; in revised form 6 January 2003)